



Published in final edited form as:

NeuroUrol Urodyn. 2013 November ; 32(8): 1130–1136. doi:10.1002/nau.22372.

Lack of Nicotinamide Mononucleotide Adenylyltransferase 2 (*Nmnat2*): Consequences for Mouse Bladder Development and Function

Amy N. Hicks*, Lysanne Campeau, David Burmeister, Colin E. Bishop, Karl-Erik Andersson
Wake Forest Institute for Regenerative Medicine, Winston Salem, North Carolina

Abstract

Aims—To describe the morphological and functional consequences for bladder development and function when nicotinamide mononucleotide adenylyltransferase 2 (*Nmnat2*) is lacking or reduced.

Methods—The Bloated Bladder (*Blad*) mouse, lacking *Nmnat2*, and heterozygotes were utilized for this investigation. Morphology and development of the bladder were studied using immunohistochemistry against urothelial, smooth muscle, and nerve markers. Functional effects were assessed by organ bath experiments and cystometry.

Results—Homozygote mutants were malformed and died at birth, whereas heterozygotes survived and morphologically did not differ from wild-type controls. Morphological bladder changes appeared in the *Blad* mutants as early as embryonic day 15.5 (E15.5) with an extremely distended bladder at E18.5. Staining revealed that all the bladder layers were present and expressed mature markers in all three genotypes. No nerves could be demonstrated by immunohistochemistry in the *Blad* mutant bladder at E18.5. Organ bath analysis showed that bladders from *Blad* mutant showed signs of denervation supersensitivity in response to carbachol, and no response to electrical stimulation of nerves at E18.5. Adult heterozygotes, which have a reduced expression of *Nmnat2* at E18.5, showed decreased responses to carbachol and electrical stimulation compared to wild-type controls. The latter also retained their ability to empty their bladders, but showed increased micturition pressures compared to controls.

Conclusions—Complete loss of *Nmnat2* leads to a mature but distended bladder in utero and is not compatible with survival. Moderate loss of *Nmnat2* has no effect on bladder development, survival, and has only modest effects on bladder function later in life.

Keywords

bladder development; bladder function; mouse mutant; *Nmnat2*; peripheral innervation

*Correspondence to: Amy N. Hicks, Wake Forest Institute for Regenerative Medicine, 391 Technology Way, Winston Salem, NC 27101. ahicks@wakehealth.edu.

Conflict of interest: none.

INTRODUCTION

In humans, the urinary bladder develops from the urogenital sinus and the surrounding splanchnic mesenchyme during the first 12 weeks of gestation, and its development is regulated by complex epithelial–mesenchymal signaling events.¹ The cranial or vesical region of the urogenital sinus will form the bladder and is attached to the allantois. The transitional epithelium develops from endoderm. The molecular signaling and developmental programs that regulate and coordinate the formation of the bladder from tissue lineages in and adjacent to the cloaca are largely unknown, including its innervation.¹ In dogs, early fetal organs are supplied only by cholinergic nerve fibers.² In the human fetal bladder at 17 weeks, a plexus of nerves containing neuropeptide Y and staining for the general nerve marker protein gene product 9.5 (PGP 9.5), was found throughout the detrusor muscle, and as gestational age increased, other peptide containing nerves (vasoactive intestinal peptide, substance P, calcitonin gene-related peptide) were observed.³ However, little is known about the development of bladder innervation and what factors are involved.

The Bloated Bladder gene trap mouse mutant,⁴ lacking *Nmnat2* (nicotinamide mononucleotide adenylyltransferase 2) may offer an opportunity to study this aspect of bladder development. *Nmnat2* is a neuron specific gene^{5–9} that has been linked with delayed Wallerian degeneration in primary sensory and sympathetic nerve cell injury models in vitro.^{7,10} Furthermore, recent information suggests that, during embryogenesis, *Nmnat2* plays an essential role in axonal maintenance.⁴ Homozygous mutant mice from the Bloated Bladder (*Blad*) mouse mutant strain lacking *Nmnat2*, at late gestation, show a greatly distended bladder, underdeveloped diaphragm and a reduction in total skeletal muscle mass. Mutant mice die perinatally, whereas heterozygotes (*Het*) appear normal, despite having only 50–75% of the *Nmnat2* amount in the brain compared to wild type at E18.5.⁴ The role for *Nmnat2* for the development of peripheral organ innervation, including the urinary bladder, is not known, nor is the consequences for the bladder when the gene is reduced or lacking.

The purpose of this study was to describe the effects of the loss of *Nmnat2* on bladder development through analysis of morphology, maturation, and function. To find out if reduced *Nmnat2* levels affect bladder function later in life, in vitro and in vivo studies were also conducted in adult *WT* and *Het* mice.

MATERIALS AND METHODS

Animals

Mouse mutants were generated at the Baylor College of Medicine as previously described.¹¹ Animals were group housed with same gender littermates unless there was a need to singly house the animal, for example, surgery. The barrier facility, where the mice were housed, is run by dedicated care staff with cage changes every 3 days, monitoring every day, and a 12-hr light–dark cycle. Every mouse in the study was genotyped for the presence of the transposon insertion in the *Nmnat2* gene as previously described.⁴ For the developmental studies, seven timed pregnant females (three for histology and four for organ bath) were utilized. For the adult cystometry and organ bath studies, three complete litters containing a total of 20 mice (11 *Het* and 9 *WT*, weighing 25.9–48.2 g) were utilized.

All experiments were carried out in accordance with recommendations from the Guide for the Care and Use of Laboratory Animals of the National Institutes of Health. The Wake Forest University Laboratory Animal Care and Use Committee approved the animal protocol (Permit Number: A11-037). All efforts were made to minimize the suffering of the animals. Both CO₂ and cervical dislocation were utilized to euthanize.

Histology

Whole embryos were fixed in 4% paraformaldehyde in PBS overnight, processed, embedded in paraffin and then cut into 7 μ m sagittal slices. Slides were cleared in xylene and rehydrated to water where they were ready for either immunohistochemistry or Hematoxylin and Eosin staining.

Immunohistochemistry

For immunohistochemistry, a separate group of whole E18.5 and E13.5 embryos were processed as described above. For labeling peripheral axons, we employed a rabbit polyclonal antibody against PGP9.5 (AbD Serotec 7863-0504, 1:3,000). To label the urothelial layer a rabbit polyclonal antibody against Uroplakin III (Abcam # ab82173, 1:2,000) was utilized. Lastly, to examine the development of the detrusor muscle rabbit polyclonal antibodies against Smooth Muscle α -actin (Abcam # ab5694, 1:200), Desmin (Abcam # ab15200, 1:300), and smooth muscle Myosin Heavy Chain 2 (Abcam # ab53219, 1:100) were used. A biotinylated anti-rabbit IgG secondary antibody (Vector BA-1000, 1:300) and DAB were used to visualize the localization of the primary antibodies. Hematoxylin was used as a counterstain before the sections were cleared in xylene and cover slipped with MM24 mounting medium (Leica Biosystems, Wetzlar, Germany).

Organ Bath Experiments

Fetuses were harvested at E18.5 from the mother, and immediately placed in ice-cold Krebs buffer. Each fetus remained in oxygenated Krebs solution during excision of the bladder. The location of the bladder was identified using a dissection microscope, and it was excised down to the bladder neck. The whole bladder was pinned at either end, and knots were made at the bladder dome and the bladder neck with 5-0 silk sutures. The lower suture was attached to a tissue holder, and the upper suture was attached to a force transducer as part of an organ bath system (Danish Myo Technology, Aarhus, Denmark) containing 15 ml of Krebs buffer aerated with 95% O₂/5% CO₂ at 37°C. The bladders were subjected to a resting tension of 0.25 g and allowed to stabilize for at least 60 min. Tissues were then primed with 60 mM KCl-induced contractions (recorded as changes in tension from baseline) and repeated until subsequent contractions were consistent. Carbachol (CCh) concentration response curves were generated with increasing concentrations of CCh at $\frac{1}{2}$ log increments starting at 3 nM up to 100 μ M. A single 1 μ M dose of ATP was given to induce purinergic-mediated contraction. For the electrical field stimulation (EFS) protocol, tissue was placed between two platinum electrodes in the organ chamber, and electrical pulses (0.5 msec pulse width, 20 V in the bath) were delivered, lasting 30 sec at increasing frequencies (1, 2, 4, 8, 16, and 32 Hz) using a S88 stimulator (Grass Instruments, W Warwick, RI). All tissue responses were normalized to grams of tissue weight.

Adult bladders were isolated after cystometry experiments were completed. Bladders were carefully extracted before the trigone and dome were removed. The tissue was then cut into two strips and hooked on either end before being hung up in the same organ bath apparatus utilized for the embryo bladder studies. One strip was used for the pharmacological stimuli as described in the embryo study, and the other strip was utilized for the EFS studies. In addition to the EFS protocol described above, 1 μM atropine, 100 μM suramin, or 1 μM tetrodotoxin (TTX) were added before generation of different EFS frequency–response curves. For each treatment, the drug was incubated with the tissue for 30 min before EFS and washed out afterwards. TTX was the last treatment added.

Cystometry Experiments

Surgical procedures—A total of 21 mice, aged 4–13 months (25.9–48.2 g body weight), were investigated (12 heterozygotes and 9 wild-type mice). Mice were anesthetized with isoflurane and the abdomen was opened by a lower midline incision. The bladder and urethra were identified and separated free from surrounding tissues. A polyethylene catheter (PE-10 intramedic polyethylene catheter (Becton-Dickinson, Sparks, MD) with cuff was inserted into the bladder dome and anchored with a purse-string silk suture. The catheter was tunneled subcutaneously and exited through an incision made at the back of the animal's neck. Ketoprofen was utilized as an analgesic post-surgery to alleviate discomfort.

Cystometric evaluation—Cystometric evaluation was performed on freely moving conscious animals 3 days after bladder catheter implantation. The previously implanted bladder catheter was connected to a 3-way valve that is, in turn, connected to a pressure transducer and an infusion pump. The pressure transducer was connected to an ETH 400 (CD Sciences, Dover, N Hampshire) transducer amplifier and subsequently connected to a MacLab/8e (Analog Digital Instruments, Castle Hill, New South Wales, Australia) data acquisition board. The pressure transducers and acquisition board were calibrated in centimeters of water before each experiment. Room temperature saline was infused at a stable rate of 1.5 ml/hr. Micturition volumes were measured with a silicone-coated funnel leading into a collection tube which was connected to a force displacement transducer. Analysis begun after a consistent voiding pattern was established. The following cystometric parameters were investigated: basal pressure (BP, lowest pressure between voids), maximum pressure (MP, the highest bladder pressure during micturition), threshold pressure (TP, pressure which initiates a voiding contraction), intermicturition pressure (IMP, mean bladder pressure between voids), bladder capacity (B_{cap}), hourly infused volume divided by the frequency of micturition per hour), micturition volume (MV, volume voided), residual volume (RV, bladder capacity-micturition volume), bladder compliance ($B_{\text{com}} = B_{\text{cap}} / (TP - BP)$), and area under the (pressure) curve between two micturitions (AUC), as a proxy for non-voiding contractions. AUC is a calculated integral that correlates with overall bladder pressures between voiding contractions and has no particular threshold.

Statistics

Either a 1-way or 2-way ANOVA statistical analysis was utilized on all of the organ bath analysis with a Bonferroni correction. IBM SPSS Statistics 19 software was used to compare the cystometric parameters. Comparisons of the cystometric values between the phenotypes

were performed using a two-tailed Student's *t*-test of independent samples. A 95% confidence interval was established and a *P*-value below 0.05 was considered significant. For all of the studies other than the cystometry analysis, males and females were combined for the analysis due to low animal numbers, but all of the changes were in the same direction for both genders.

RESULTS

Gross Anatomy

After opening the abdomen of the E18.5 *WT* and *Blad* mutant, it was observed that the latter had an extremely distended and full bladder (Fig. 1A). Pressure applied to the abdomen resulted in a release of fluid from the urethral opening, indicating that the urethra was patent at full term. This phenotype became externally observable at E15.5 with a slightly hunched body shape that was more severe at E18.5, but any differences in general body shape were undetectable at E13.5. Differences in body shape and posture of the *WT* and *Het* mice were undetectable at all observed time points.

Histology and Immunohistochemistry

Immunohistochemistry for PGP9.5 demonstrated nerves within the *WT* and *Het* bladder, but no nerve structures were found in the *Blad* mutant bladder (Fig. 1B). At E13.5, structures related to the urogenital sinus, urethra, and distal part of the hind gut were all visible in embryos from all three genotypes (Fig. 2). By E15.5, the *Blad* mutants appeared to have a smaller, hypertrophied bladder compared with their *WT* and *Het* littermates (Fig. 2). Once the embryos reached full term development at E18.5, the *WT* and *Het* bladders appeared to be normal and fully developed while the *Blad* mutant bladder was extremely distended. Serial sections through the lower portion of the urogenital tract did not reveal any indication of a blockage. Both the detrusor smooth muscle, urothelial and lamina propria layers were clearly visible, but extremely thin as shown in a higher magnification image of the *Blad* mutant bladder wall (Figs. 2 and 3).

Immunohistochemistry of the detrusor smooth muscle showed that smooth muscle α -actin, smooth muscle myosin heavy chain 2 (MHC2), and desmin were detectable in all three genotypes (Fig. 3), indicating that the detrusor smooth muscle expresses mature markers. Also, uroplakin 3 (UPK3) staining indicated the presence of mature urothelial umbrella cells in the *Blad* mutant bladder wall (Fig. 3).

Organ Bath Experiments

Embryo development—None of the *Blad* mutant bladders at E18.5 ($n = 8$) responded to EFS (Fig. 4A). At this time point, five out of nine *Het* bladders and two of three *WT* bladders investigated responded to electrical stimulation. However, all groups responded to stimulation with the muscarinic receptor agonist carbachol (Fig. 4B), the purinergic agonist ATP, and to depolarization with KCl. The maximum contraction to carbachol was significantly higher in *Blad* and *Het* than in *WT* bladders ($WT E_{\max} = 90.6 \pm 9.1$, $Het E_{\max} = 178.0 \pm 19.5$, and $Blad E_{\max} = 253.4 \pm 23.6$) (Fig. 4C). However, only the EC_{50} value of the *Blad* mutant bladder ($EC_{50} = -5.7 \pm 0.1$) was significantly ($P < 0.01$) different from

those of *WT* and *Het* mice with no differences between the *Het* ($EC_{50} = -4.995 \pm 0.1$) and *WT* ($EC_{50} = -4.965 \pm 0.1$) bladders (Fig. 4D), suggesting denervation supersensitivity only in the *Blad* mutants. The amplitude of the response to 60 mM KCl and 1 mM ATP was not statistically different amongst all three genotypes.

Adult/aging—As shown in Figure 5A, the dose–response curve to carbachol stimulation was depressed in *Het* mice compared to *WT* animals, both at 4–6 and at 13 months. The E_{max} values were significantly lower in the *Het* bladder strips (61.9 ± 9.1 at 4–6 months and 75.4 ± 7.1 at 13 months) than in the *WT* bladders (109.7 ± 9.8 at 4–6 months and 114.8 ± 5.3 at 13 months) at both time points (Fig. 5B). The responses to EFS at 4–6 months were not significantly different in the *Het* than in the *WT* bladders. However, significant differences were found at 13 months at higher frequencies (Fig. 5C). TTX eliminated all responses to EFS.

Cystometric Studies

Twelve *Het* mice and nine *WT* mice aged 4–13 months were investigated. Significantly higher values for TP (27.4 ± 2.0 cm H₂O vs. 21.5 ± 1.8 cm H₂O), IMP (15.1 ± 1.0 cm H₂O vs. 11.1 ± 1.3 cm H₂O), and AUC (15.5 ± 1.0 vs. 12.1 ± 1.0) were found in the *Het* mice compared to the *WT*. Other cystometric parameters did not differ. When the seven *Het* males were compared with the four male *WT* separately, significant differences were found for IMP (14.5 ± 0.9 cm H₂O vs. 10.9 ± 0.9 cm H₂O), AUC (14.9 ± 0.9 vs. 11.4 ± 0.9), and RV (0.18 ± 0.01 cm H₂O vs. 0.09 ± 0.02 cm H₂O). No such differences were found in females.

DISCUSSION

The Bloated Bladder (*Blad*) mouse model provides an interesting opportunity to study how the bladder develops in the absence of innervation. The timing of the initiation of axonal degeneration suggests that the peripheral nerves either never forms a functional muscular contact or that they only form one for a very insignificant amount of time. Our organ bath studies on E18.5 *Blad* mutant bladders showed unresponsiveness to EFS stimulation and signs of denervation supersensitivity, which seems to confirm this hypothesis. The bladder wall itself appeared to develop, mature, and retain function even in the absence of innervation during development.

In humans, bladder smooth muscle has been reported to form between 7 and 12 weeks of gestation.¹² There is a difference in timing of bladder organogenesis between different species, for example, rats, rabbits, mice, and humans.¹³ In mice, bladder development and smooth muscle differentiation occurs between E13 and E18.^{12,14,15} Urethral development begins at E10.25 after the genital tubercle development is initiated when paired buds of lateral plate mesoderm come from underneath the ventral wall ectoderm on either side of the cloaca, in a proximal to distal outgrowth. The urethral plate then canalizes to form a urethral tube.¹⁶ Thus, in humans, the bladder forms in the first trimester, whereas, in mice, the bladder forms at the beginning of the third trimester. Such differences may limit the generalizability of animal experiments to human development, but the mouse model still can provide important translational information.¹⁵

Differentiation of bladder smooth muscle involves a complex array of local environmental factors, epithelial–mesenchymal interactions, and signaling pathways. An epithelial signal is necessary to induce smooth muscle differentiation in the adjacent bladder mesenchyme. For example, sonic hedgehog (Shh), which is expressed by the urothelium, promotes mesenchymal proliferation and induces differentiation of smooth muscle from embryonic bladder mesenchyme.^{16,17} The role of bladder nerves for detrusor smooth muscle development has not been established. In the *Blad* mouse, we found that the bladder did show some hypertrophy at E15.5 and was extremely distended at full term. The reasons for this can only be speculated on. The urethra was patent on histological assessment, so we could not demonstrate evidence of urethral obstruction at the time-points examined, which could have been a plausible cause. If the bladder were extremely compliant and lacking intrinsic tone, mechanical forces from urine production could result in bladder distension. Interestingly, the distended bladder from *Blad* mice showed greater contractile strength at E18.5 in response to cholinergic stimuli compared to *WT* and *Het* animals. Moreover, mutant bladders exhibited decreased EC₅₀ values after cholinergic stimulation, suggesting denervation supersensitivity. Mutant bladders also responded to ATP, suggesting that even in the absence of nerves, there was a development of functional purinergic receptors.

Nmnat2 has been linked to axonal maintenance.⁴ Without *Nmnat2*, axons develop all the way out to the peripheral tissues up to E13.5 but then degenerate and disappear by full term (E18.5). E13.5 is the time point when nerves begin to form muscular connections. While the exact mechanism by which *Nmnat2* helps to maintain axons during development is not understood, it is clear that degeneration is initiated between E13.5 and E15.5. The smaller hypertrophied bladder at E15.5, followed by an extremely distended thin bladder at E18.5, could be related to the lack of innervation observed, or to aberrant urethral development such as delayed canalization that might have occurred at different time-points of embryonic development than those examined histologically. Interestingly, even though there is a 50–75% decrease in *Nmnat2* expression in the *Het* mice at E18.5, there were no differences in the lumbar motoneuron and sensory neurons in the dorsal root ganglion compared to their *WT* littermates, and axons were detectable in the hind limb of the *Het* mice at all embryonic time points.⁴

Since *Nmnat2* has also been tied to tauopathy associated neurodegeneration and progression of Alzheimer's disease,^{7,18} it was a natural leap to see if there were signs of neurodegeneration in the bladder with age. Expression of *Nmnat2* in adult brains showed a trend of reduced expression in the *Het* animals at all ages in this study that is consistent with the E18.5 results (data not shown). There was a modest reduction in the response to EFS stimulation in *Het* mice, but a significant reduction in the maximal contractile response to carbachol at all time points. In the cystometric experiments on animals aged 4–13 months, *Het* mice exhibited higher TP, IMP, and AUC than their *WT* controls, but also an increased RV in males. These findings would suggest that higher pressures are generated in the *Het* mice during micturition (TP) in order to overcome an increased bladder outlet resistance. As we do not study sphincter electromyography or pressure–flow curves, we cannot determine the differences in bladder outlet resistance. It may be speculated that over time, these higher pressures could eventually cause detrusor decompensation, as sometimes seen in other neuropathic bladders. This would be in agreement with the reduced responses to EFS and

carbachol in the adult *Het* bladders as well as the early over compensation that is illustrated by the increased E18.5 *Het* E_{max} . The reduced responsiveness in the *Het* bladder tissue is either due to decreased functionality of the nerves or a reduction in the number of nerves innervating the tissues, but this is a continued area of research for this mouse mutant.

CONCLUSIONS

The *Blad* mouse mutant shows the importance of fetal bladder nerve development for normal bladder function. Lack of *Nmnat2* and the absence of nerves do not seem to prevent the development of a mature bladder wall that is responsive to transmitters mediating bladder contraction. Moderate loss of *Nmnat2* has no effect on bladder development and survival, and only modestly effects on bladder function later in life.

ACKNOWLEDGMENTS

We would like to thank Brandi Bickford in the Wake Forest Virtual Microscopy Core for her assistance with slide scanning, and Cathy Mathis for her expertise and advice on the histology experiments. We would also like to acknowledge the trouble shooting assistance of Drs. Masanori Nomiya and Norifumi Sawada with the organ bath apparatus. Finally, we would like to cite support by NIH grant Type: U01 HD43421 to C.E.B. The funders had no role in study design, data collection and analysis, decision to publish, or preparation of the manuscript.

Grant sponsor: NIH; Grant number: U01 HD43421.

REFERENCES

1. Shapiro E. Clinical implications of genitourinary embryology. *Curr Opin Urol.* 2009; 19:427–433. [PubMed: 19461520]
2. Arrighi S, Bosi G, Cremonesi F, et al. Immunohistochemical study of the preand postnatal innervation of the dog lower urinary tract: Morphological aspects at the basis of the consolidation of the micturition reflex. *Vet Res Commun.* 2008; 32:291–304. [PubMed: 18071920]
3. Jen PY, Dixon JS, Gosling JA. Immunohistochemical localization of neuromarkers and neuropeptides in human fetal and neonatal urinary bladder. *Br J Urol.* 1995; 75:230–235. [PubMed: 7531592]
4. Hicks AN, Lorenzetti D, Gilley J, et al. Nicotinamide mononucleotide adenylyltransferase 2 (*nmnat2*) regulates axon integrity in the mouse embryo. *PLoS ONE.* 2012; 7:e47869. [PubMed: 23082226]
5. Berger F, Lau C, Dahlmann M, et al. Subcellular compartmentation and differential catalytic properties of the three human nicotinamide mononucleotide adenylyltransferase isoforms. *J Biol Chem.* 2005; 280:36334–36341. [PubMed: 16118205]
6. Raffaelli N, Sorci L, Amici A, et al. Identification of a novel human nicotinamide mononucleotide adenylyltransferase. *Biochem Biophys Res Commun.* 2002; 297:835–840. [PubMed: 12359228]
7. Yan T, Feng Y, Zheng J, et al. *Nmnat2* delays axon degeneration in superior cervical ganglia dependent on its NAD synthesis activity. *Neurochem Int.* 2010; 56:101–106. [PubMed: 19778564]
8. Mayer PR, Huang N, Dewey CM, et al. Expression, localization, and biochemical characterization of nicotinamide mononucleotide adenylyltransferase 2. *J Biol Chem.* 2010; 285:40387–40396. [PubMed: 20943658]
9. Emanuelli M, Carnevali F, Saccucci F, et al. Molecular cloning, chromosomal localization, tissue mRNA levels, bacterial expression, and enzymatic properties of human NMN adenylyltransferase. *J Biol Chem.* 2001; 276:406–412. [PubMed: 11027696]
10. Gilley J, Coleman MP. Endogenous *Nmnat2* is an essential survival factor for maintenance of healthy axons. *PLoS Biol.* 2010; 8:e1000300. [PubMed: 20126265]

11. Wang B, Harrison W, Overbeek PA, et al. Transposon mutagenesis with coat color genotyping identifies an essential role for Skor2 in sonic hedgehog signaling and cerebellum development. *Development*. 2011; 138:4487–4497. [PubMed: 21937600]
12. Baskin LS, Hayward SW, Sutherland RA, et al. Mesenchymal-epithelial interactions in the bladder. *World J Urol*. 1996; 14:301–309. [PubMed: 8912470]
13. Longhurst P. Developmental aspects of bladder function. *Scand J Urol Nephrol Suppl*. 2004; 215:11–19.
14. Baskin LS, Hayward SW, Young P, et al. Role of mesenchymal-epithelial interactions in normal bladder development. *J Urol*. 1996; 156:1820–1827. [PubMed: 8863624]
15. Tasian G, Cunha G, Baskin L. Smooth muscle differentiation and patterning in the urinary bladder. *Differentiation*. 2010; 80:106–117. [PubMed: 20541860]
16. Perriton CL, Powles N, Chiang C, et al. Sonic hedgehog signaling from the urethral epithelium controls external genital development. *Dev Biol*. 2002; 247:26–46. [PubMed: 12074550]
17. Shiroyanagi Y, Liu B, Cao M, et al. Urothelial sonic hedgehog signaling plays an important role in bladder smooth muscle formation. *Differentiation*. 2007; 75:968–977. [PubMed: 17490411]
18. Ljungberg MC, Ali YO, Zhu J, et al. CREB-activity and nmnat2 transcription are down-regulated prior to neurodegeneration, while NMNAT2 over-expression is neuroprotective, in a mouse model of human tauopathy. *Hum Mol Genet*. 2012; 21:251–267. [PubMed: 22027994]

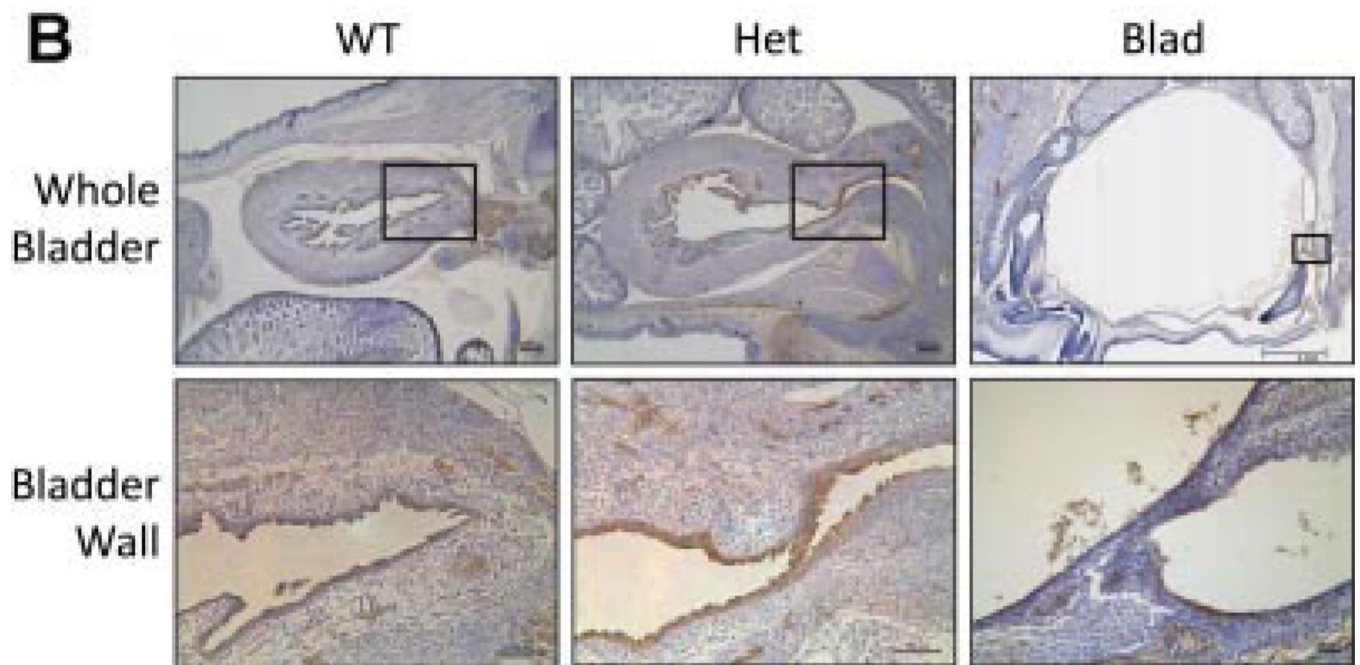


Fig. 1. Bladder distension and innervation in the *Blad* mouse mutant. **A:** E18.5 *WT* and *Blad* littermates opened up to show the distended and full bladder in the *Blad* mutant compared to the *WT*. **B:** Sagittal sections of *WT*, *Het*, and *Blad* E18.5 embryos stained for PGP9.5 showing both the whole bladder and a close up of the bladder wall. The black box on the image of the whole bladder indicates the location of the higher magnification image. Whole bladder *WT* and *Het* imaged at 5 \times magnification, and *Blad* imaged at 1.25 \times . Bladder wall images taken at 10 \times for the *WT* and *Het* and at 40 \times for the *Blad* image. Image 1A from Hicks et al.⁴ with permission.

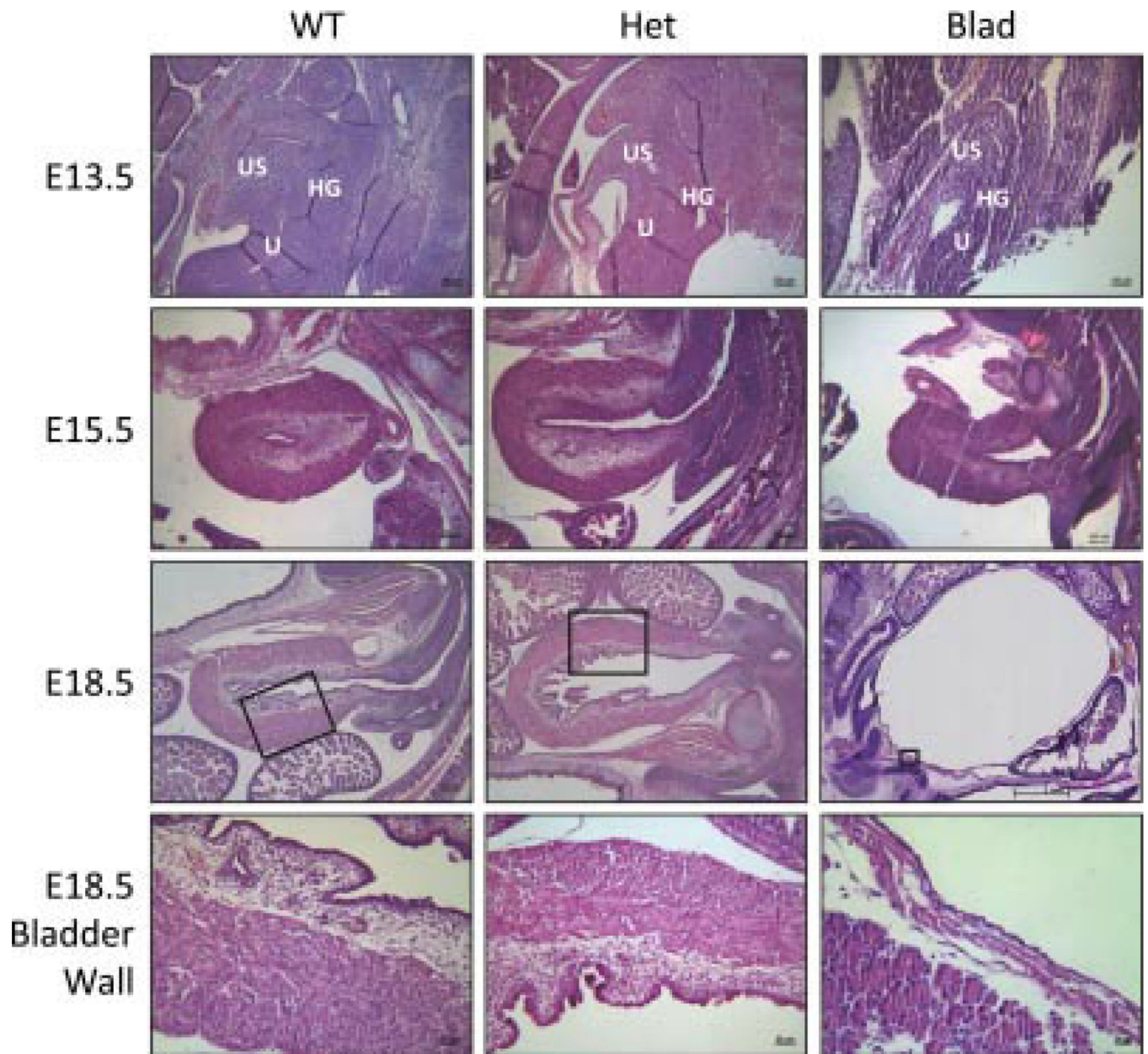


Fig. 2. Bladder morphology during development. Hematoxylin and eosin stained sagittal sections of *WT*, *Het*, and *Blad* embryos at E13.5, E15.5, and E18.5. The black box on the image of the E18.5 whole bladder indicates the location of the higher magnification image. All E13.5 and E15.5 images were taken at 10× magnification. E18.5 *WT* and *Het* bladders were imaged at 5× for the whole bladder and 20× to show the bladder wall where E18.5 *Blad* images were taken at 1.25× and 40×, respectively. US, urogenital sinus; U, urethra; HG, distal part of the hind gut.

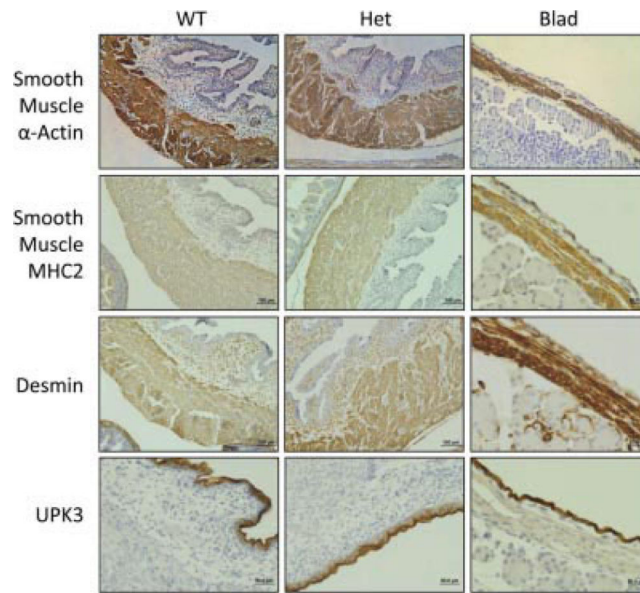


Fig. 3. Bladder wall developmental markers. Immunohistochemistry stained E18.5 sagittal sections of *WT*, *Het*, and *Blad* littermates showing the bladder wall stainings for smooth muscle α -actin, smooth muscle myosin heavy chain 2 (MHC2), desmin, and uroplakin 3 (UPK3). All *WT* and *Het* images taken at a 20 \times magnification while the *Blad* images were taken at 40 \times .

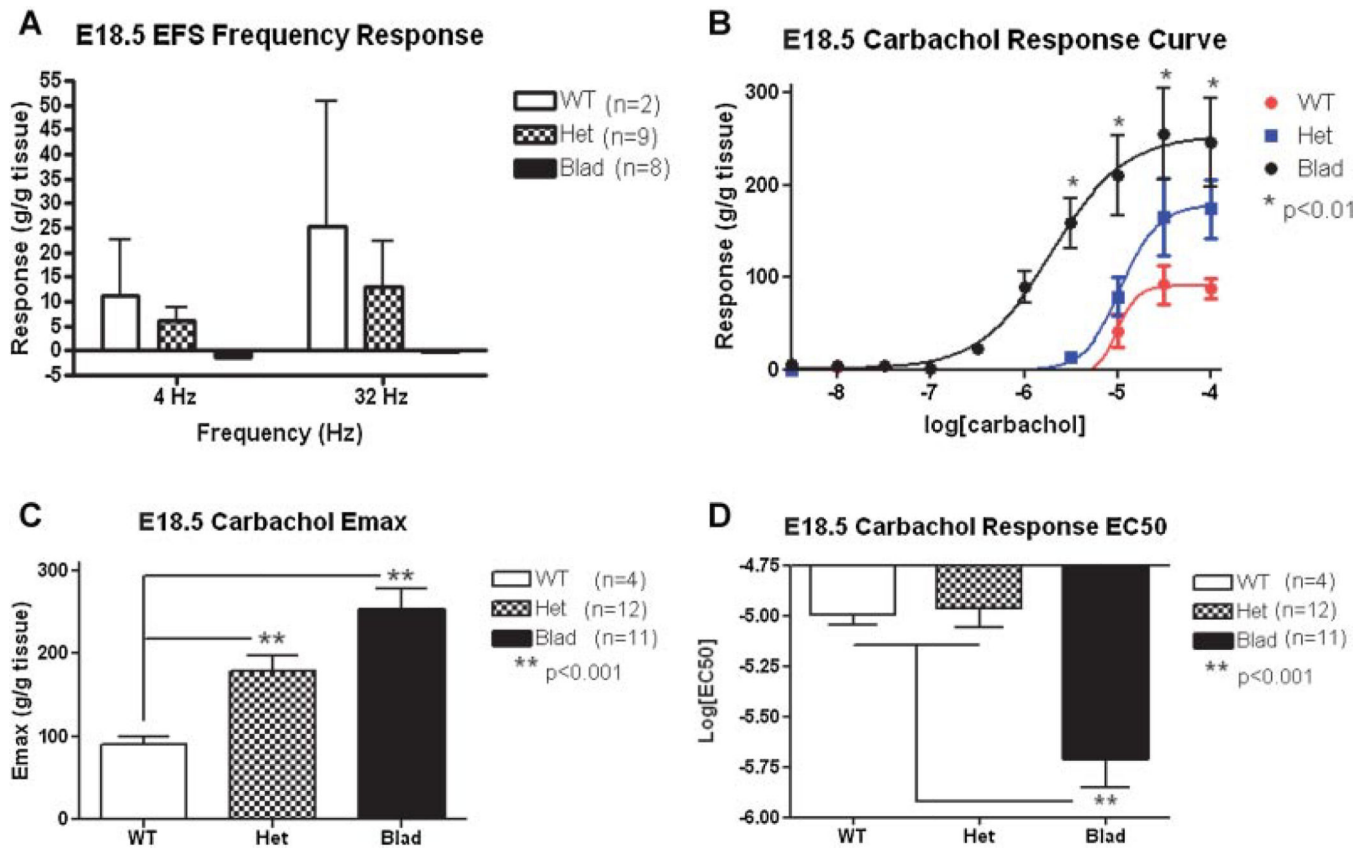


Fig. 4. EFS and carbachol dose-responses at E18.5. This analysis was done on whole bladders from E18.5 *WT* (white/red), *Het* (checkered/blue), and *Blad* (black) littermates. **A:** Graph of EFS frequency responses for all three genotypes at both 4 and 32 Hz. **B:** Carbachol dose-response curve with a linear regression. **C:** Maximum contraction (E_{max}) of each genotype bladder to carbachol stimulation. The difference between the *Het* and *Blad* E_{max} was also significant with $P < 0.02$. **D:** EC_{50} values (the concentration of carbachol that produces 50% of the total contraction) for each genotype. A 2-way ANOVA with a Bonferroni correction was utilized for statistical analysis of the carbachol response curve and a 1-way ANOVA was used for the E_{max} and EC_{50} . Error bars represent the standard deviation.

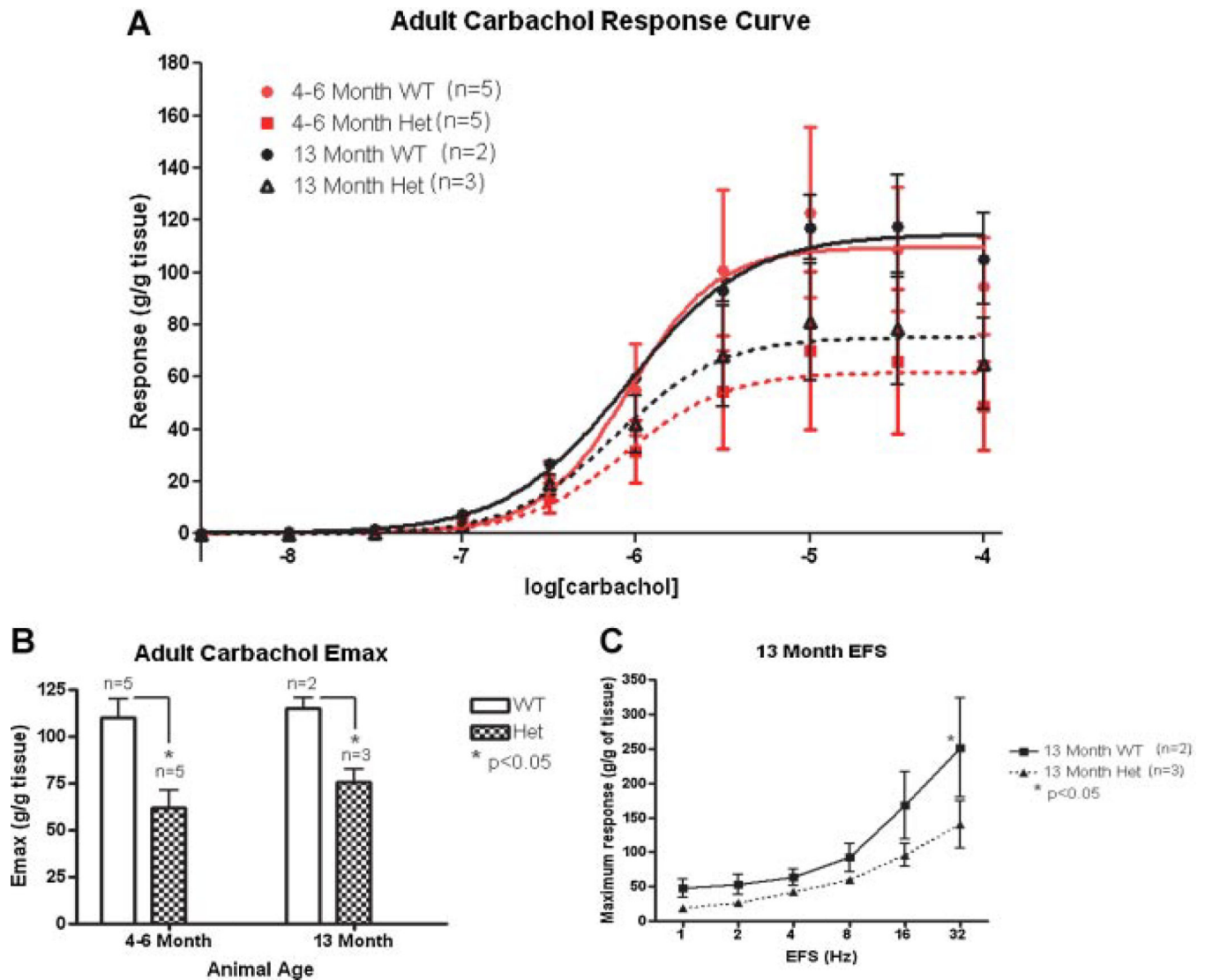


Fig. 5. Carbachol and EFS stimulation in adult animals. This analysis was done on bladder strips from 4- to 6-month (red) and 13-month (black) old *WT* (solid line) and *Het* (dotted line) animals. **A:** Carbachol dose–response curve. **B:** Maximum contraction (E_{max}) of each genotype after carbachol stimulation. **C:** Frequency–response to electric field stimulation (EFS) on 13-month-old bladders. A 2-way ANOVA with a Bonferroni correction was utilized for statistical analysis of the carbachol response curve/EFS frequency–response and a 1-way ANOVA was used for the E_{max} . Error bars represent the standard deviation.